Journal of Magnetic Resonance 219 (2012) 75–82

Contents lists available at SciVerse ScienceDirect

Journal of Magnetic Resonance

journal homepage: www.elsevier.com/locate/jmr

Heteronuclear Adiabatic Relaxation Dispersion (HARD) for quantitative analysis of conformational dynamics in proteins

Nathaniel J. Traaseth [a,e], Fa-An Chao [a], Larry R. Masterson [a], Silvia Mangia [c], Michael Garwood [c], Shalom Michaeli [c], Burckhard Seelig [a,d], Gianluigi Veglia [a,b,*]

[a] Department of Biochemistry, Molecular Biology, and Biophysics, University of Minnesota, Minneapolis, MN 55455, United States
[b] Department of Chemistry, University of Minnesota, Minneapolis, MN 55455, United States
[c] Department of Radiology (Center for Magnetic Resonance Research), University of Minnesota, Minneapolis, MN 55455, United States
[d] BioTechnology Institute, University of Minnesota, St. Paul, MN 55108, United States
[e] Department of Chemistry, New York University, New York, NY 10003, United States

ARTICLE INFO

Article history:
Received 31 July 2011
Revised 22 March 2012
Available online 6 April 2012

Keywords:
Adiabatic relaxation dispersion
Rotating frame relaxation
NMR
Proteins

ABSTRACT

NMR relaxation methods probe biomolecular motions over a wide range of timescales. In particular, the rotating frame spin-lock $R_{1\rho}$ and Carr–Purcell–Meiboom–Gill (CPMG) R_2 experiments are commonly used to characterize μs to ms dynamics, which play a critical role in enzyme folding and catalysis. In an effort to complement these approaches, we introduced the Heteronuclear Adiabatic Relaxation Dispersion (HARD) method, where dispersion in rotating frame relaxation rate constants (longitudinal $R_{1\rho}$ and transverse $R_{2\rho}$) is created by modulating the shape and duration of adiabatic full passage (AFP) pulses. Previously, we showed the ability of the HARD method to detect chemical exchange dynamics in the fast exchange regime ($k_{ex} \sim 10^4$–10^5 s^{-1}). In this article, we show the sensitivity of the HARD method to slower exchange processes by measuring $R_{1\rho}$ and $R_{2\rho}$ relaxation rates for two soluble proteins (ubiquitin and 10C RNA ligase). One advantage of the HARD method is its nominal dependence on the applied radio frequency field, which can be leveraged to modulate the dispersion in the relaxation rate constants. In addition, we also include product operator simulations to define the dynamic range of adiabatic $R_{1\rho}$ and $R_{2\rho}$ that is valid under all exchange regimes. We conclude from both experimental observations and simulations that this method is complementary to CPMG-based and rotating frame spin-lock $R_{1\rho}$ experiments to probe conformational exchange dynamics for biomolecules. Finally, this approach is germane to several NMR-active nuclei, where relaxation rates are frequency-offset independent.

1. Introduction

Proteins exist as structural ensembles [1,2], whose *conformational dynamics* reflect a fine balance between the enthalpic and entropic contributions to the free energy. While enthalpy is relatively easy to access *via* thermocalorimetric measurements, the estimate of conformational entropy is more difficult to obtain. Yet, the entropic contribution has been postulated to be the driving force for phenomena such as protein folding, ligand binding, cooperativity, and allostery. In the past decades, there has been an enormous effort to quantify the conformational entropy contribution to the overall entropy for enzymes [1–10]. NMR has an important niche in structural biology since it can give site-specific dynamic information in a non-invasive manner. Not only do NMR relaxation experiments reveal protein motions (dynamics) on a wide range of timescales from ps to ms [11–13], they do so from an atomic perspective for both protein backbone and sidechain nuclei [14]. In particular, the motions on the μs to ms timescale are receiving special attention since they often occur on the same timescale as catalysis and folding [15]. Remarkably, these motions dictate substrate recognition, ligand positioning within the active site, product release in enzymatic catalysis [1,7,8,16–19], and more recently have been directly linked to the chemical step of catalysis [20]. A fascinating aspect recently discovered is the possibility of converting the information derived from relaxation measurements to the characterization of *excited states* [21] (partially folded or under conformational strain) that are often responsible for the biological activity of soluble [5] and membrane-bound proteins [22–25]. Although always present in the NMR measurements, these states were previously undetected in simple analyses of NMR spectra.

Abbreviations: HARD, Heteronuclear Adiabatic Relaxation Dispersion; CPMG, Carr–Purcell–Meiboom–Gill; $R_{1\rho}$, longitudinal rotating frame relaxation rate constant; $R_{2\rho}$, transverse rotating frame relaxation rate constant.

* Corresponding author. Address: 6-155 Jackson Hall, 321 Church St. SE, Minneapolis, MN 55455, United States. Fax: +1 612 625 2163.
E-mail address: vegli001@umn.edu (G. Veglia).

1090-7807/$ - see front matter © 2012 Elsevier Inc. All rights reserved.
http://dx.doi.org/10.1016/j.jmr.2012.03.024

The classical methods to determine molecular motions in the μs to ms timescale are spin-lock $R_{1\rho}$ and Carr–Purcell–Meiboom–Gill (CPMG) R_2 experiments [15]. Dispersion of relaxation rates for CPMG and spin-lock $R_{1\rho}$ are generated by changing the effective radio frequency (RF) field (in $R_{1\rho}$ experiment) or the spacing between the 180° refocusing pulses (in CPMG) [26]. More recently a new variant of these methods referred to as *divided evolution* has been added [27] that allows one to quantify msec chemical exchange by manipulating the peak position rather than the relaxation rate.

As a *complement* to the above methods, we recently obtained relaxation dispersion by modulating the shape and duration of adiabatic full passage (AFP) pulses, i.e. Heteronuclear Adiabatic Relaxation Dispersion (HARD) [28]. AFP pulses [29] are routinely used in NMR imaging for measuring $R_{1\rho}$ and $R_{2\rho}$ relaxation rate constants. A similar method was first introduced by Konrat and Tollinger to measure $R_{1\rho}$ rates that were converted to R_2 relaxation rates and also shown to have minimal offset dependence [30]. Unlike the latter approach, the HARD method uses a series of AFP pulses of the hyperbolic secant family (HSn) to measure transverse (HARD-$R_{2\rho}$ experiment) or longitudinal (HARD-$R_{1\rho}$ experiment) rotating frame relaxation rate constants during adiabatic rotations of the ^{15}N magnetization. The pulses are applied in groups of four and cycled using MLEV-4 [31]. At the end of every four pulses, transverse (for $R_{2\rho}$) or longitudinal (for $R_{1\rho}$) magnetization remains. As a model system, we used ^{15}N labeled ubiquitin and acquired two datasets at 5 °C and 25 °C [28], demonstrating that the HARD method qualitatively probes motions on the fast exchange NMR timescale. The primary advantage of adiabatic over square pulses is the ability to induce effective rotation angles that do not vary over a large frequency bandwidth. Moreover, simulations and experimental tests carried out on model compounds (e.g., ethanol/water mixtures) show that the dispersion obtained with adiabatic pulses is nominally sensitive to the maximum $\omega_1^{\max}/(2\pi)$ RF pulse amplitude [32,33], opening up the possibility of tuning the effective RF frequency to modulate the extent of the relaxation dispersion phenomena.

In this article, we demonstrate the ability of the HARD method to detect protein motions both in the μs and ms timescales, with a direct comparison with the well-established CPMG and $R_{1\rho}$ experiments. Through the introduction of a quantitative fitting procedure for extracting the exchange parameters and product operator simulations, we outline the dynamic range for detecting internal dynamics in biomolecular systems.

2. Results

2.1. Effect of radio frequency amplitude in the HARD method

To analyze the effect of the RF field strength for the HARD method on biomolecules, we measured $R_{1\rho}$ and $R_{2\rho}$ relaxation rates at $\omega_1^{\max}/(2\pi) = 3, 4,$ and 5kHz maximal applied amplitude of the AFP pulses. The results are shown in Fig. 1. For all residues in ubiquitin that undergo chemical exchange (Ile23, Asn25, Thr55, and Val70), the dispersion in $R_{2\rho}$ (i.e., difference between HS1 and HS8) is noticeably smaller at 3 and 4 kHz than at 5 kHz. For example, Asn25 has dispersions of 4.7 s^{-1}, 5.6 s^{-1}, and 7.8 s^{-1} at RF pulse amplitudes of 3 kHz, 4 kHz, and 5 kHz, respectively. Here, we have used the AFP pulses of the hyperbolic secant family, HSn, where n = 1, 2, 4, 6, and 8 are the stretching factors for the AFP pulses. The difference plot ($\Delta R_{2\rho} = R_{2\rho,\mathrm{HS1}} - R_{2\rho,\mathrm{HS8}}$) for HARD-$R_{2\rho}$ in Fig. 2 also indicates that the largest dispersion was generated with $\omega_1^{\max}/(2\pi) = 5$ kHz. Due to the smaller contribution of R_2 to the observed relaxation rates, the $R_{1\rho}$ experiment is essentially insensitive to the RF field strength as shown in Fig. 2 (i.e., dispersion changes between 3 and 5 kHz is <1 s^{-1}). This shows that while the HARD method can accurately detect exchange, it is more sensitive when $\omega_1^{\max}/(2\pi) \geqslant 4$ kHz.

2.2. Quantitative interpretation of dynamic parameters from adiabatic $R_{1\rho}$ and $R_{2\rho}$

The dynamic parameters including k_{ex} (=$1/\tau_{ex}$) and $\Delta\omega^2 p_A p_B$ were extracted by considering the averaged instantaneous contribution of the exchange throughout the course of AFP by integrating the expressions below [28]:

$$R_{1\rho,\mathrm{ex}} = \frac{1}{T_p}\int_0^{T_p} p_A p_B \Delta\omega^2 \sin^2\alpha(t)\frac{\tau_{ex}}{1+(\omega_{\mathrm{eff}}(t)\tau_{ex})^2}dt \quad (1)$$

$$R_{2\rho,\mathrm{ex}} = \frac{1}{T_p} \times \int_0^{T_p} p_A p_B \Delta\omega^2\left[\cos^2\alpha(t)\tau_{ex} + 1/2\sin^2\alpha(t)\frac{\tau_{ex}}{1+(\omega_{\mathrm{eff}}(t)\tau_{ex})^2}\right]dt \quad (2)$$

where $\Delta\omega$ is the chemical shift difference between magnetic sites A and B, α is the angle between the effective frequency (ω_{eff}) and the B_0 magnetic field, p_A and p_B are fractional populations for a two-site chemical exchange process, and T_p is the adiabatic full passage pulse length. Eqs. (1) and (2) were derived in the fast exchange regime [32], where the condition $\omega_{\mathrm{eff}}\,\tau_{ex} \ll 1$ is well satisfied [34]. During the adiabatic full passage, both α and ω_{eff} are time dependent. To obtain only the contribution of the exchange term to the measured relaxation rate, we subtracted rates from residues that did not show chemical exchange from those that did [28]. This assumption relied on the fact that all the other contributions to the measured relaxation rate other than chemical exchange were the same. Auer et al. recently showed that the chemical shift anisotropy-dipole coupling (CSA-DD) cross-correlated relaxation rate was the most important factor when fitting adiabatic $R_{1\rho}$ relaxation dispersion data [35]. Therefore to address our assumption, we measured these relaxation rates for ubiquitin [58]. As is shown in Supporting Information Fig. 1, the cross-relaxation rates for ubiquitin (outside of the termini) vary by ~±1 s^{-1} across the primary sequence. This small difference is essentially outside the experimental error of the approach and suggests that in the case of ubiquitin CSA-DD cross-correlated relaxation can be neglected among different residues.

In order to determine whether a residue in ubiquitin has dispersion by our HARD method, we calculated $\Delta R_{1\rho}$ ($R_{1\rho,\mathrm{HS8}} - R_{1\rho,\mathrm{HS1}}$) and $\Delta R_{2\rho}$ ($R_{2\rho,\mathrm{HS1}} - R_{2\rho,\mathrm{HS8}}$) and plotted the results as a function of residue (Fig. 2). In the absence of exchange (or for exchange rates that are outside the detection limits) the $\Delta R_{1\rho}$ and $\Delta R_{2\rho}$ values will be similar for each residue. Those residues with greater than one standard deviation (excluding termini) were deemed to have anisochronous exchange (i.e., exchange between spins with different chemical shifts). To obtain only the chemical exchange relaxation contribution, the relaxation rates of non-exchanging adjacent residues were averaged and then subtracted from the exchanging residue. For example, to calculate the exchange contribution for Asn25, the $R_{1\rho}$ and $R_{2\rho}$ rates of residues 20, 21, 22, 26, 27, and 28 were first averaged and then subtracted from the observed rates measured for Asn25. This yielded data that contained only the exchange contribution that can be directly fit using Eqs. (1) and (2) to obtain k_{ex} and $\Delta\omega^2 p_A p_B$. Using this approach, we report the fitted curves in Fig. 3 and the kinetic parameters in Table 1, which are in excellent agreement with those reported by Palmer and co-workers [36] and Griesinger and co-workers [44] for ubiquitin. This close agreement with literature values and the small

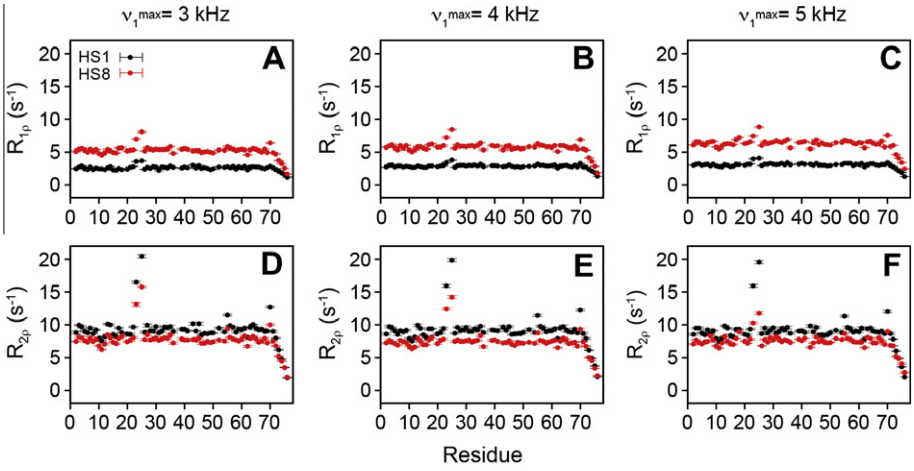

Fig. 1. Adiabatic HS1 and HS8 $R_{1\rho}$ (A–C) and $R_{2\rho}$ (D–F) relaxation rates measured for ubiquitin at 5 °C as a function of the maximum applied RF field $\upsilon_1^{max} = \omega_1^{max}/(2\pi)$ of 3 kHz (A and D), 4 kHz (B and E), and 5 kHz (C and F). HS1 and HS8 pulses are black and red, respectively as indicated in the legend. Each adiabatic pulse was 4 ms in length and executed in blocks of four to give total relaxation delays of 16, 32, 48, 64, 80, 96, and 128 ms for $R_{1\rho}$ and 16, 32, 48, 64, 80, and 96 ms for $R_{2\rho}$. Relaxation rates were obtained from single exponential fits using 2D peak intensities from these datasets.

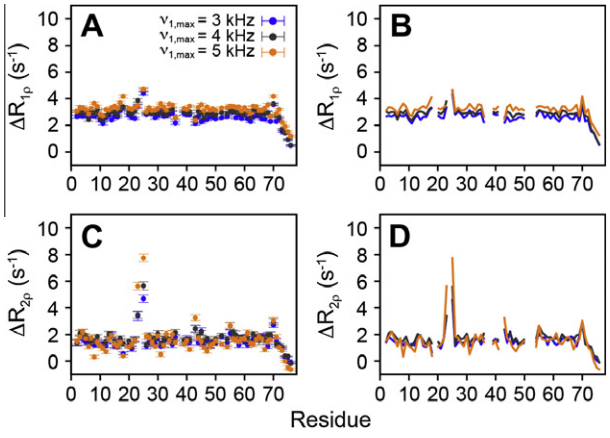

Fig. 2. (A) $\Delta R_{1\rho}$ ($=R_{1\rho,HS8} - R_{1\rho,HS1}$) and (C) $\Delta R_{2\rho}$ ($=R_{2\rho,HS1} - R_{2\rho,HS8}$) calculated from data in Fig. 1 as a function of the maximal RF applied amplitude. A residue that shows a value outside one standard deviation was considered to have a relaxation contribution due to chemical exchange (R_{ex}). To better observe the trend, we have plotted the line graph of the same data in panels B ($\Delta R_{1\rho}$) and D ($\Delta R_{2\rho}$). As indicated in the legend, υ_1^{max} values of 3, 4, and 5 kHz correspond to blue, gray, and orange.

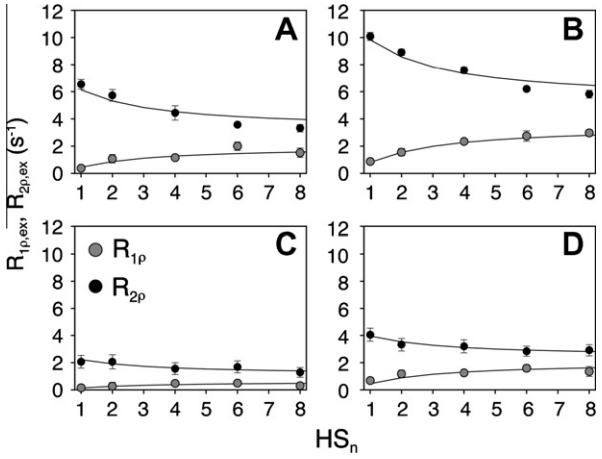

Fig. 3. Fitted HARD dispersion curves measured for [U-^{15}N] ubiquitin at 5 °C for υ_1^{max} = 3.5 kHz [28]. Panels A, B, C, and D correspond to residues 23, 25, 55, and 70, respectively. The relaxation contribution from chemical exchange only is shown, and was derived by subtracting the relaxation rates of non-exchanging residues from those that have an exchange contribution. The parameters from the fit are reported in Table 1.

variance of the CSA/DD transverse cross-relaxation rates as a function of residue provides further support that the subtraction approach is an accurate way to determine the chemical exchange contribution in the HARD method.

2.3. Comparison of HARD method with CPMG relaxation dispersion

Ubiquitin is a good model sample for fast exchange rates, with $k_{ex} \sim 10^4\ s^{-1}$ [28,36]. While the motions occurring on this timescale are important for catalysis and folding [3,4], slower timescales have been the subject of several studies aimed at measuring conformational exchange in signaling enzymes and other macromolecules [1,7,20,37–39]. For these experiments, CPMG-based R_2 experiments are typically employed, which are generally sensitive to exchange rate constants in the 10^2–$10^4\ s^{-1}$ range. To investigate this exchange regime, we used an artificially evolved RNA ligase enzyme [40]. This primordial enzyme was engineered to ligate a 5′-triphosphate activated RNA to the terminal 3′-hydroxyl of a second RNA molecule, a function that has not been found in nature. We first performed CPMG relaxation dispersion experiments on the RNA ligase

Table 1
Simultaneous fitting of Eqs. (1) and (2) to obtain k_{ex} and $\Delta\omega^2 p_A p_B$ values for each residue. The exchange contribution was obtained by the subtraction method for data obtained at υ_1^{max} = 3.5 kHz [28]. The non-exchanging residues listed in parentheses were averaged and subsequently subtracted from the following exchanging residues: Ile23 (20, 21, 22, 26, 27, 28), Asn25 (20, 21, 22, 26, 27, 28), Thr55 (51, 52, 54, 56, 57, 58), and Val70 (66, 67, 68, 69, 71, 72). $\Phi_{ex} = \Delta\omega^2 p_A p_B$. Error bars result from jackknife simulations using repeated relaxation rates determined from HS1 pulses. The Massi et al. values were obtained at 280 K [36], the Ban et al. values at 277 K [44], and the values from this work (Traaseth et al.) at 278 K.

	Traaseth et al.	Massi et al. [36]	Ban et al. [44]
Residue	k_{ex} ($10^4\ s^{-1}$)		
Ile23	2.2 ± 0.1	2.32 ± 0.27	1.2 ± 0.3
Asn25	2.4 ± 0.1	2.32 ± 0.22	1.4 ± 0.1
Thr55	1.9 ± 0.2	2.5 ± 0.6	–
Val70	3.8 ± 0.3	2.6 ± 0.4	1.5 ± 0.2
	Φ_{ex} (10^4 rad^2 s^{-2})		
Ile23	15 ± 1	8.1 ± 1.0	11.3 ± 4.1
Asn25	27 ± 1	15.9 ± 2.2	18.5 ± 2.2
Thr55	4.8 ± 0.6	4.1 ± 1.2	–
Val70	17 ± 1	5.9 ± 0.9	5.4 ± 1.4

at 20 °C and found that several residues had dispersion in relaxation rates > 5 s^{-1} ($\nu_{CPMG,50Hz} - \nu_{CPMG,1000Hz}$). We then collected full adiabatic $R_{1\rho}$ and $R_{2\rho}$ datasets. The results are shown in Fig. 4 and Supporting Information Fig. 2 (data are divided into separate panels). From this set of experiments, the residues with the largest dispersions for adiabatic $R_{2\rho}$ were 28, 49, 50, 51, 68, and 69, which is in good agreement with the CPMG experiments. To identify whether slower exchange processes could be probed using standard approaches, we performed the off-resonance spin-lock $R_{1\rho}$ experiment as described previously [36,41]. This experiment was used to compare our method for ubiquitin in our previous work [28]. From Fig. 5, CPMG and the HARD $R_{2\rho}$ experiments sensitively detect the exchange process occurring in the RNA ligase, while the spin-lock $R_{1\rho}$ experiment is only slightly sensitive. The CPMG experiment gave a larger dispersion than did the adiabatic $R_{2\rho}$ experiment. However, the HARD-$R_{2\rho}$ experiment was able to detect μs to ms dynamics in both faster (ubiquitin) and slower exchange processes (RNA ligase), whereas the CPMG experiment could not sensitively detect exchange in ubiquitin [28].

2.4. Dynamic range of adiabatic $R_{1\rho}$ and $R_{2\rho}$ versus CPMG and spin-lock $R_{1\rho}$

The range of conformational dynamics within biopolymers covers vibrational motions of chemical bonds to large amplitude domain rearrangements. Nuclear spin relaxation experiments can be tailored to detect motions occurring from psec to msec timescales [15]. For RNA ligase and ubiquitin, we showed that it is possible to set the window of detection by choosing experimental parameters such as echo time used in CPMG and ω_1^{max} in the adiabatic pulses for $R_{1\rho}$ and $R_{2\rho}$. To better define the dynamic range covered by the above experiments, we carried out computational simulations for a two-site exchange system under anisochronous exchange. The calculations were performed using a random exchange process combined with product operator formalism [42,43]. This approach is applicable to any pulse sequence that utilizes both hard and shaped pulses. We consider the simple case of two-site exchange at equilibrium between specific magnetic sites A and B with the direct and backwards exchange rate constants k_A and k_B ($k_{ex} = k_A + k_B$) coupled through the Bloch-McConnell relationship: $k_A/p_B = k_B/p_A$, where p_A and p_B are the normalized equilibrium populations ($p_A + p_B = 1.0$). The method used in this work was described in detail in [43]. These simulations make it possible to calculate the trajectories of the density matrix evolution in the presence of exchange:

$$\sigma_k(t) = \prod e^{-iH_i\Delta t_i}\sigma_k(0)\prod e^{iH_i\Delta t_i} \quad (3)$$

where H_i is the time-dependent Hamiltonian and $\sigma(t)$ is the density matrix. The calculations were performed by simulating 1000 randomly distributed evolution trajectories by creating random intervals between jumps for the exchange process [43]. To simulate the dynamic range covered by each method in a similar manner as that shown for the experimental data in Figs. 2 and 5, we calculated the relaxation dispersion observed in the simulations as follows: CPMG, $\Delta R_{2eff} = R_{2eff,\nu CPMG=50Hz} - R_{2eff,\nu CPMG=1000Hz}$; HARD-$R_{2\rho}$, $\Delta R_{2\rho} = R_{2\rho,HS1} - R_{2\rho,HS8}$; HARD-$R_{1\rho}$, $\Delta R_{1\rho} = R_{1\rho,HS8} - R_{1\rho,HS1}$; spin-lock $R_{1\rho}$, $\Delta R_{2eff} = R_{2eff,\nu eff=1500Hz} - R_{2eff,\nu eff=2870Hz}$. In accordance with experimental findings reported by Palmer and co-workers [36], we set $\Delta\nu = 600$ Hz ($\Delta\nu = \Delta\omega/2\pi$) and $p_A = 0.97$. The simulation results in Fig. 7 show that maximal relaxation dispersion is obtained for CPMG and HARD-$R_{2\rho}$ experiments at k_{ex} values of ~1000–7000 s^{-1} and ~2500–8500 s^{-1}, respectively. On the other hand, the maximal dispersion of spin-lock $R_{1\rho}$ falls in the range of 4500–10,500 s^{-1}. In our simulations, we observed the smallest dispersion for the HARD-$R_{1\rho}$ method. However, this experiment probes the fastest exchange rates and has the broadest sensitivity range with similar dispersions from $k_{ex} \sim 15{,}000$ to 50,000 s^{-1}. For ubiquitin, the simulations are in strong agreement with the experimental values reported in Table 1 [36,44]. Specifically, the highlighted region in Fig. 7B corresponds to the k_{ex} values we obtained for ubiquitin (20,000–30,000 s^{-1}) [28]. The simulations confirm our experimental findings that the HARD-$R_{2\rho}$ experiment gives the largest relaxation dispersion over this range of k_{ex}. In general, the HARD-$R_{2\rho}$ or HARD-$R_{1\rho}$ experiments provide the largest dispersions ranging from ~10^4–10^6 s^{-1} under these simulation parameters. While these differences are somewhat small (~2 s^{-1}), this further validates our experimental results on ubiquitin [28] and establishes the HARD method as an alternative experiment that can complement existing nuclear relaxation experiments. Furthermore, it should be noted that by increasing the applied field strength of the adiabatic pulses (Figs. 1 and 2) it is possible to induce even larger dispersions.

One of the benefits of the HARD method is that the $R_{1\rho}$ and $R_{2\rho}$ experiments displayed differential sensitivity to the exchange process (Figs. 6 and 7). Therefore, when both HARD-$R_{1\rho}$ and HARD-$R_{2\rho}$ show relaxation dispersion, data can be fit simultaneously as shown in Fig. 3 for ubiquitin. This reduced the ambiguity of the fitted parameters and improved the reliability of the fit in a similar manner as dispersion curves acquired at two or more magnetic field strengths [45,46]. While additional data at a second magnetic field strength would further improve reliability of the fitted data shown in Table 1, this may not be required of the HARD method. For RNA ligase, the simulations agree well with the experimental results that suggest the motion is too slow to be probed using HARD-$R_{1\rho}$ or spin-lock-$R_{1\rho}$ with the given experimental parameters (e.g., effective spin-lock field strength). Note that while we show fitted RNA ligase $R_{2\rho}$ dispersion curves in Fig. 6, a second magnetic field is required to obtain reliable fitted parameters, similar to the spin-lock-$R_{1\rho}$ and CPMG relaxation dispersion experiments. Furthermore, future developments are needed to investigate new fitting approaches that apply to slower exchange processes, since the formalism in Eqs. (1) and (2) apply only to the fast exchange regime.

Based on the above computational results, we conclude that (a) the simulations corroborate the experimental data for ubiquitin and RNA ligase and (b) the HARD method is a good complement to the existing methods for characterizing conformational dynamics.

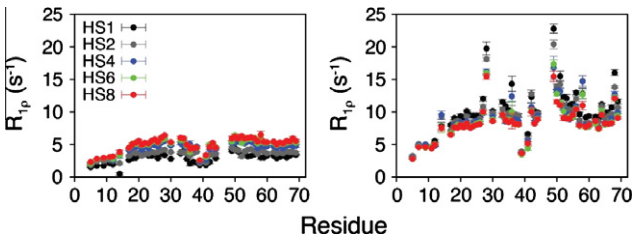

Fig. 4. HARD $R_{1\rho}$ (left) and $R_{2\rho}$ (right) relaxation rates measured for the RNA ligase at 20 °C. The HSn pulses are color-coded as indicated in the legend. Each adiabatic pulse was 4 ms in length and executed in blocks of four to give total relaxation delays of 16, 32, 48, 64, 80, 96, and 112 ms for $R_{1\rho}$ and 16, 32, 48, 64, 80, 96, and 112 ms for $R_{2\rho}$. Relaxation rates were obtained from single exponential fits using 2D peak intensities from these datasets. Supporting Information Fig. 2 shows the same data in separate panels.

3. Discussion

Adiabatic pulses have been powerful tools to observe contrast in magnetic resonance imaging (MRI) [33,47,48] and to assess spin dynamics of cerebral metabolites in the human brain [49]. For

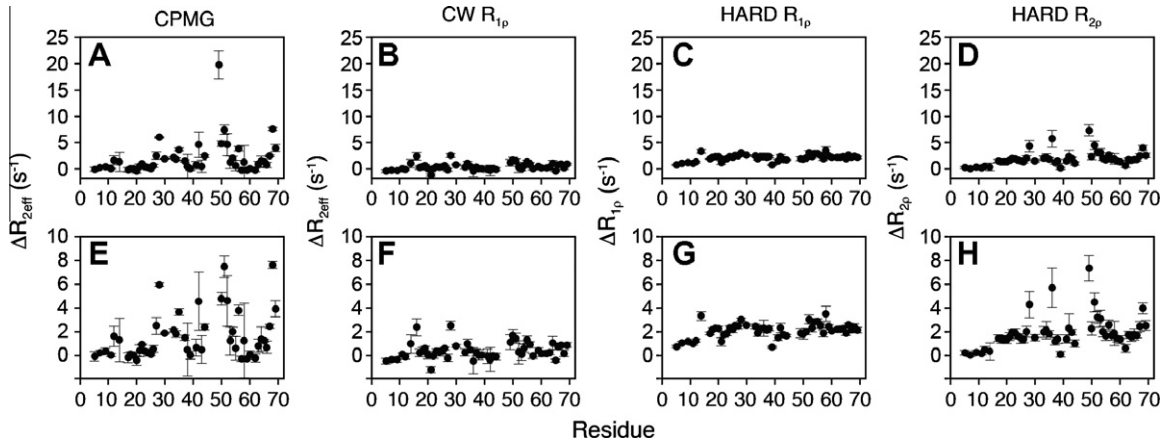

Fig. 5. Comparison of CPMG (A and E), spin-lock $R_{1\rho}$ (B and F), HARD $R_{1\rho}$ (C and G) and $R_{2\rho}$ (D and H) relaxation rates measured for the RNA ligase at 20 °C. All values are delta plots defined as the difference between the end-points in each of the experiments. For the HARD method it is $\Delta R_{1\rho}$ ($=R_{1\rho,HS8} - R_{1\rho,HS1}$) and $\Delta R_{2\rho}$ ($=R_{2\rho,HS1} - R_{2\rho,HS8}$), for CPMG it is ΔR_{2eff} ($=R_{2eff,\nu CPMG=50Hz} - R_{2eff,\nu CPMG=1000Hz}$), and for spin-lock $R_{1\rho}$ it is ΔR_{2eff} ($R_{2eff,\omega eff\sim1500Hz} - R_{2eff,\omega eff\sim2900Hz}$). Note for spin-lock $R_{1\rho}$ each residue is slightly different due to the dependence on the frequency offset. The top and bottom rows are the same data with different *y*-axis scales. Due to this, residue 49 data in panel E is cut-off and does not appear. The relatively large error bars in the CPMG experiment for some residues in panel E are due to low signal intensity in the 2D spectra, presumably from the 40 ms of constant time used in the experiment.

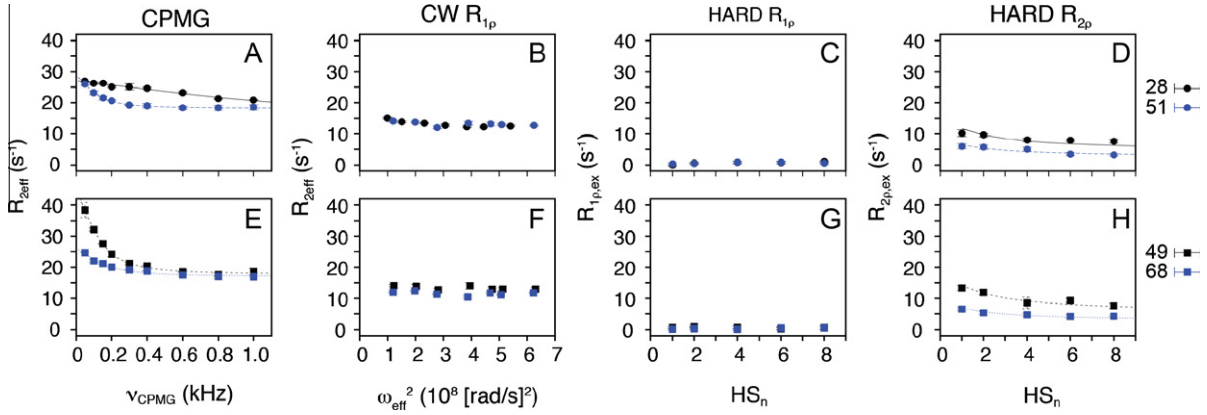

Fig. 6. Dispersion curves of four residues (28, 49, 51, and 68) in RNA ligase that showed a chemical exchange contribution to the observed relaxation rates. The CPMG data are shown in A and E, the spin-lock $R_{1\rho}$ data in B and F, the HARD $R_{1\rho}$ data in C and G, and the HARD $R_{2\rho}$ data in D and H. The top panels are for residues 28 (black) and 51 (blue), while the bottom panels show residues 49 (black) and 68 (blue). The exchange contribution of residues 28, 49, 51, and 68 for HARD $R_{1\rho,ex}$ and $R_{2\rho,ex}$ was obtained by subtracting the average relaxation rates from residues 20–25 (non-exchanging residues). Since the $R_{1\rho}$ HARD experiment did not show exchange (panels C and G), all values of $R_{1\rho,ex}$ were set to 0 for the fitting of the k_{ex} values using Eqs. (1) and (2). The fits shown in panels D and H yielded similar k_{ex} values for all residues (average of 3900 Hz with standard deviation of 1600 Hz). Fitted k_{ex} values from the CPMG experiment were 900 ± 200 s^{-1} (average ± standard deviation) for residues 49, 51, and 68, while residue 28 yielded an exchange rate of 6500 s^{-1}. These values are obtained from data acquired at only one magnetic field (14.1 T). (For interpretation of the references to color in this figure legend, the reader is referred to the web version of this article.)

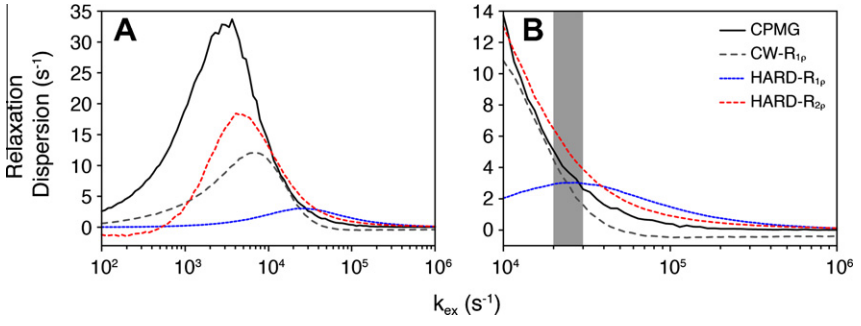

Fig. 7. Product operator simulations defining the dynamic range of the four experimental methods investigated in this article to measure relaxation dispersion. These simulations are valid over all exchange regimes (i.e., all k_{ex} values). The difference between exchange-induced relaxation rate constants obtained with different parameters of CPMG, adiabatic $R_{1\rho}$ and $R_{2\rho}$, and spin-lock $R_{1\rho}$ methods. The method used in this work was described previously [43]. For CPMG, ΔR_{2eff} ($R_{2eff,\nu CPMG=50Hz} - R_{2eff,\nu CPMG=1000Hz}$); for adiabatic methods the $\Delta R_{2\rho}$($=R_{2\rho,HS1} - R_{2\rho,HS8}$) and $\Delta R_{1\rho}$ ($=R_{1\rho,HS8} - R_{1\rho,HS1}$) using $\nu_{1,max}$ = 4 kHz, and spin-lock $R_{1\rho}$, ΔR_{2eff} ($R_{2eff,\nu eff=1500Hz} - R_{2eff,\nu eff=2870Hz}$). Other parameters were $\Delta\nu$ = 600 Hz and p_A = 0.97. Panel B is the same data as panel A with a change in the displayed *x* and *y* scales. The gray region corresponds to the k_{ex} values of ubiquitin reported in Table 1.

these experiments, RF power deposition and time of acquisition are at a premium due to the requirements of working with live samples. Our aim is to integrate a wide variety of adiabatic pulse modulation functions in order to increase the dynamic range and to make relaxation measurements more feasible for macromolecules. There are several parameters that can be varied to improve the performance of the HARD method. For example, carrying out the adiabatic $R_{1\rho}$ and $R_{2\rho}$ experiments with $\omega_1^{max}/(2\pi)$ set to 5 kHz increased the dispersion by ~60–70% in ubiquitin. While this applied RF amplitude may exceed current cryogenic probe technology, room temperature probes are capable of handling these powers. Improvements in hardware are expected to make these techniques applicable for large molecules that benefit from sensitivity increases from cryogenic probes. In addition, development of new adiabatic pulses that satisfy *superadiabatic* conditions would further advance the HARD method [50]. We also outlined a fitting strategy to extract dynamic parameters that were in excellent agreement with literature values of ubiquitin without the need to back-calculate rates in a frequency-dependent manner.

If the inherent exchange parameters are optimally sensitive for the CPMG experiment (see Fig. 5), larger relaxation dispersions were obtained relative to the HARD method. Nevertheless, for faster exchange processes, the adiabatic $R_{1\rho}$ and $R_{2\rho}$ experiments were more sensitive than the CPMG-based experiment [28]. The simulations in Fig. 7 corroborate the experimental results, showing that the HARD experiments ($R_{1\rho}$ and $R_{2\rho}$) gave the largest relaxation dispersion from k_{ex} 10^4–10^6 s^{-1}.

Although our simulations used only one set of parameters common to proteins (p_A, p_B, $\Delta\omega$, radiofrequency pulse amplitude, and pulse durations), we observed that adiabatic $R_{2\rho}$ detects slightly faster processes than CPMG. In addition, the adiabatic $R_{2\rho}$ experiment significantly reduced the measured relaxation rates as compared to the free precession R_2 CPMG experiment, which allowed for greater signal to noise. HARD-$R_{1\rho}$, however, is able to detect even faster processes than HARD-$R_{2\rho}$, essentially those timescales covered by spin-lock $R_{1\rho}$. This complements the existing approaches by giving greater flexibility in choosing an appropriate and sensitive experiment for quantifying conformational exchange.

In summary, the HARD method uses adiabatic pulses that cover a large bandwidth and give reliable rate constants over the entire spectral width. In addition, HARD is a complementary approach that can be used if CPMG-based and rotating frame spin-lock $R_{1\rho}$ techniques are not sensitive for a particular sample (e.g., short T_2 times). This method can be further improved by innovations that select long-lived coherences (shorter relaxation rates) [51] and advancements in NMR hardware (ultrafast timescale resolution and improved power handling) that will further extend the dynamic range for probing motions at all timescales.

4. Materials and methods

4.1. Sample preparation

^{15}N-labeled ubiquitin was grown in *Escherichia coli* BL21(DE3) and purified using size-exclusion chromatography. The sample was ~1 mM. The expression and purification of the RNA ligase will be published elsewhere. The sample for testing the HARD method consisted of ~1 mM RNA ligase in 20 mM HEPES, 150 mM NaCl, 10 mM β-mercaptoethanol, ~2 mM $ZnCl_2$, and at a pH = 7.5.

4.2. NMR spectroscopy

All experiments were performed on Varian spectrometers (INOVA and VNMRS) operating at a ^{1}H frequency of 600 MHz. The experiments on ubiquitin were performed at 5 °C as described previously [28], while those with the RNA ligase were carried out at 20 °C. Adiabatic pulses of the HSn variety were used, where n = 1, 2, 4, 6, and 8. In the frequency modulated (FM) frame, the amplitude and frequency modulated functions for the HS1 pulse are given by [52]:

$$\omega_1(t) = \omega_1^{max}\,\mathrm{sech}(\beta(2t/T_p - 1)) \tag{4}$$

$$\omega_{RF}(t) - \omega_c = A\tanh(\beta(2t/T_p - 1)) \tag{5}$$

For the HSn pulse with n > 1:

$$\omega_1(t) = \omega_1^{max}\,\mathrm{sech}(\beta(2t/T_p - 1)^n) \tag{6}$$

$$\omega_{RF}(t) - \omega_c = A\int \mathrm{sech}^2(\beta\tau^n)d\tau \tag{7}$$

where $t \in [0, T_p]$, $\tau = 2t/T_p - 1$ and $|\tau| \leqslant 1$ for $t \in [0, T_p]$, β is a truncation factor ($\mathrm{sech}(\beta) = 0.01$), A is the amplitude of the frequency sweep in rad/s, T_p is pulse length, ω_c is carrier frequency (the center frequency in the bandwidth of interest), and ω_1^{max} is the maximum value of $\omega_1(t)$.[1] For our experiments, T_p was set to 4 ms. Total relaxation delays were 16, 32, 48, 64, 80, 96, and 128 ms for $R_{1\rho}$ and 16, 32, 48, 64, 80, and 96 ms for $R_{2\rho}$ experiments. The 2D peak intensities were fit to a single exponential function to obtain the relaxation rate constant for each HSn experiment.

For ubiquitin, the adiabatic experiments were carried out with 4 scans, 80 increments in the ^{15}N dimension (spectral width of 2200 Hz), 1000 points in the ^{1}H dimension (spectral width of 12,019 Hz), and a recycle delay of 2.5–3 s. For the RNA ligase, the experiments were performed with 8 scans, 64 increments in the ^{15}N dimension (spectral width of 1600 Hz), 2048 points in the ^{1}H dimension (spectra width of 12,019 Hz), and a recycle delay of 2 s.

The CPMG experiments on the RNA ligase were performed with the pulse scheme described in Loria et al. [53], with a constant-time block of 40 ms and CPMG frequencies of 50, 100, 200, 300, 400, 600, 800, and 1000 Hz. The R_{2eff} was calculated using the reference spectrum with no constant time delay, according to the relationship:

$$R_{2eff} = \frac{-\ln(I_{\nu CPMG})}{I_0}\frac{1}{T} \tag{8}$$

where I_{CPMG} is the intensity for a given value of ν_{CPMG}, I_0 is the intensity of the reference spectrum, and T is the constant time delay. The CPMG data for RNA ligase were fit using the fast-exchange equation [54].

The spin-lock $R_{1\rho}$ off-resonance experiments [36,41] were performed on the RNA ligase using the following applied field strengths (Hz)/^{15}N offsets (Hz): 1500/475, 1500/−325, 1500/−1425, 2100/−325, 2100/−1425, 2900/−825, and 2900/−1425. These values were converted into $\overline{R}_2$ rates by considering the nominal effective field without time dependence, according to the relationship:

$$R_{1\rho} = \overline{R}_1\cos^2\alpha + \overline{R}_2\sin^2\alpha \tag{9}$$

The tanh/tan adiabatic half passage pulses [55,56] were 6 ms and utilized a 25 kHz frequency sweep [41,57]. $\overline{R}_1$ relaxation rate constants for ubiquitin and RNA ligase were measured using relaxation delays of 10, 30, 50, 200, 500, and 1000 ms. $\overline{R}_{2eff}$ was calculated from $\overline{R}_1$ values and is equal to $\overline{R}_2^0 + \overline{R}_{ex}$, where $\overline{R}_2^0$ is the rate constant originating from relaxation other than chemical exchange and $\overline{R}_{ex}$ is the relaxation rate constant from exchange. All

[1] Eq. (7) replaces Eq. (1) in [28], which was typographically incorrect. Also, the Glu24 residue previously reported in Fig. 2 [28] should have Ile23.

relaxation rate constants R_i were obtained by fitting the data to a single exponential delay ($e^{-R_i t}$) with the first point in the series of the experiment acquired twice to estimate the experimental error.

Acknowledgment

This work was supported by National Institutes of Health Grants GM072701 (G.V.), BTRR – P41 RR008079 (CMRR), R01NS061866 (S.M.), NASA Astrobiology Institute NNX09AH70A (B.S.).

Appendix A. Supplementary material

Supplementary data associated with this article can be found, in the online version, at http://dx.doi.org/10.1016/j.jmr.2012.03.024.

References

[1] D.D. Boehr, D. McElheny, H.J. Dyson, P.E. Wright, The dynamic energy landscape of dihydrofolate reductase catalysis, Science 313 (2006) 1638–1642.
[2] B. Ma, R. Nussinov, Enzyme dynamics point to stepwise conformational selection in catalysis, Curr. Opin. Chem. Biol. 14 (2010) 652–659.
[3] K.K. Frederick, M.S. Marlow, K.G. Valentine, A.J. Wand, Conformational entropy in molecular recognition by proteins, Nature 448 (2007) 325–329.
[4] M.S. Marlow, J. Dogan, K.K. Frederick, K.G. Valentine, A.J. Wand, The role of conformational entropy in molecular recognition by calmodulin, Nat. Chem. Biol. 6 (2010) 352–358.
[5] D.M. Korzhnev, T.L. Religa, W. Banachewicz, A.R. Fersht, L.E. Kay, A transient and low-populated protein-folding intermediate at atomic resolution, Science 329 (2010) 1312–1316.
[6] D. Kern, E.Z. Eisenmesser, M. Wolf-Watz, Enzyme dynamics during catalysis measured by NMR spectroscopy, Methods Enzymol. 394 (2005) 507–524.
[7] L.R. Masterson, C. Cheng, T. Yu, M. Tonelli, A.P. Kornev, S.S. Taylor, G. Veglia, Dynamics connect substrate recognition to catalysis in protein kinase A, Nat. Chem. Biol. 6 (2010) 821–828.
[8] D. Kern, E.R. Zuiderweg, The role of dynamics in allosteric regulation, Curr. Opin. Struct. Biol. 13 (2003) 748–757.
[9] H. Beach, R. Cole, M.L. Gill, J.P. Loria, Conservation of mus-ms enzyme motions in the apo- and substrate-mimicked state, J. Am. Chem. Soc. 127 (2005) 9167–9176.
[10] N. Trbovic, J.H. Cho, R. Abel, R.A. Friesner, M. Rance, A.G. Palmer 3rd, Protein side-chain dynamics and residual conformational entropy, J. Am. Chem. Soc. 131 (2009) 615–622.
[11] R. Ishima, D.A. Torchia, Protein dynamics from NMR, Nat. Struct. Biol. 7 (2000) 740–743.
[12] A.G. Palmer 3rd, Nmr probes of molecular dynamics: overview and comparison with other techniques, Annu. Rev. Biophys. Biomol. Struct. 30 (2001) 129–155.
[13] L.E. Kay, NMR studies of protein structure and dynamics, J. Magn. Reson. 173 (2005) 193–207.
[14] V. Tugarinov, L.E. Kay, Relaxation rates of degenerate 1H transitions in methyl groups of proteins as reporters of side-chain dynamics, J. Am. Chem. Soc. 128 (2006) 7299–7308.
[15] A.G. Palmer 3rd, C.D. Kroenke, J.P. Loria, Nuclear magnetic resonance methods for quantifying microsecond-to-millisecond motions in biological macromolecules, Methods Enzymol. 339 (2001) 204–238.
[16] D.D. Boehr, R. Nussinov, P.E. Wright, The role of dynamic conformational ensembles in biomolecular recognition, Nat. Chem. Biol. 5 (2009) 789–796.
[17] D.D. Boehr, D. McElheny, H.J. Dyson, P.E. Wright, Millisecond timescale fluctuations in dihydrofolate reductase are exquisitely sensitive to the bound ligands, Proc. Natl. Acad. Sci. USA 107 (2010) 1373–1378.
[18] K.A. Henzler-Wildman, M. Lei, V. Thai, S.J. Kerns, M. Karplus, D. Kern, A hierarchy of timescales in protein dynamics is linked to enzyme catalysis, Nature 450 (2007) 913–916.
[19] M.J. Carroll, R.V. Mauldin, A.V. Gromova, S.F. Singleton, E.J. Collins, A.L. Lee, Evidence for dynamics in proteins as a mechanism for ligand dissociation, Nat. Chem. Biol. 8 (2012) 246–252.
[20] G. Bhabha, J. Lee, D.C. Ekiert, J. Gam, I.A. Wilson, H.J. Dyson, S.J. Benkovic, P.E. Wright, A dynamic knockout reveals that conformational fluctuations influence the chemical step of enzyme catalysis, Science 332 (2011) 234–238.
[21] G. Bouvignies, P. Vallurupalli, D.F. Hansen, B.E. Correia, O. Lange, A. Bah, R.M. Vernon, F.W. Dahlquist, D. Baker, L.E. Kay, Solution structure of a minor and transiently formed state of a T4 lysozyme mutant, Nature 477 (2011) 111–114.
[22] N.J. Traaseth, G. Veglia, Probing excited states and activation energy for the integral membrane protein phospholamban by NMR CPMG relaxation dispersion experiments, Biochim. Biophys. Acta 1798 (2010) 77–81.
[23] K.N. Ha, N.J. Traaseth, R. Verardi, J. Zamoon, A. Cembran, C.B. Karim, D.D. Thomas, G. Veglia, Controlling the inhibition of the sarcoplasmic Ca2+-ATPase by tuning phospholamban structural dynamics, J. Biol. Chem. 282 (2007) 37205–37214.
[24] M. Gustavsson, N.J. Traaseth, C.B. Karim, E.L. Lockamy, D.D. Thomas, G. Veglia, Lipid-mediated folding/unfolding of phospholamban as a regulatory mechanism for the sarcoplasmic reticulum Ca(2+)-ATPase, J. Mol. Biol. 408 (2011) 755–765.
[25] M. Gustavsson, N.T. Traaseth, G. Veglia, Probing ground and excited states of phospholamban in model and native lipid membranes by magic angle spinning NMR spectroscopy, Biochim. Biophys. Acta 2012 (1818) 146–153.
[26] J.P. Loria, R.B. Berlow, E.D. Watt, Characterization of enzyme motions by solution NMR relaxation dispersion, Acc. Chem. Res. 41 (2008) 214–221.
[27] G. Bouvignies, D.F. Hansen, P. Vallurupalli, L.E. Kay, Divided-evolution-based pulse scheme for quantifying exchange processes in proteins: powerful complement to relaxation dispersion experiments, J. Am. Chem. Soc. 133 (2011) 1935–1945.
[28] S. Mangia, N.J. Traaseth, G. Veglia, M. Garwood, S. Michaeli, Probing slow protein dynamics by adiabatic R(1rho) and R(2rho) NMR experiments, J. Am. Chem. Soc. 132 (2010) 9979–9981.
[29] M. Garwood, L. DelaBarre, The return of the frequency sweep: designing adiabatic pulses for contemporary NMR, J. Magn. Reson. 153 (2001) 155–177.
[30] R. Konrat, M. Tollinger, Heteronuclear relaxation in time-dependent spin systems: (15)N-T1 (rho) dispersion during adiabatic fast passage, J. Biomol. NMR 13 (1999) 213–221.
[31] M. Levitt, R. Freeman, T. Frenkel, Broadband heteronuclear decoupling, J. Magn. Reson. 47 (1982) 328–330.
[32] S. Michaeli, D.J. Sorce, D. Idiyatullin, K. Ugurbil, M. Garwood, Transverse relaxation in the rotating frame induced by chemical exchange, J. Magn. Reson. 169 (2004) 293–299.
[33] S. Michaeli, D.J. Sorce, C.S. Springer Jr, K. Ugurbil, M. Garwood, T1rho MRI contrast in the human brain: modulation of the longitudinal rotating frame relaxation shutter-speed during an adiabatic RF pulse, J. Magn. Reson. 181 (2006) 135–147.
[34] D.G. Davis, M.E. Perlman, R.E. London, Direct measurements of the dissociation-rate constant for inhibitor-enzyme complexes via the T1 rho and T2 (CPMG) methods, J. Magn. Reson. B 104 (1994) 266–275.
[35] R. Auer, M. Tollinger, I. Kuprov, R. Konrat, K. Kloiber, Mathematical treatment of adiabatic fast passage pulses for the computation of nuclear spin relaxation rates in proteins with conformational exchange, J. Biomol. NMR 51 (2011) 35–47.
[36] F. Massi, M.J. Grey, A.G. Palmer 3rd, Microsecond timescale backbone conformational dynamics in ubiquitin studied with NMR R1rho relaxation experiments, Protein Sci. 14 (2005) 735–742.
[37] L.R. Masterson, L. Shi, E. Metcalfe, J. Gao, S.S. Taylor, G. Veglia, Dynamically committed, uncommitted, and quenched states encoded in protein kinase A revealed by NMR spectroscopy, Proc. Natl. Acad. Sci. USA 108 (2011) 6969–6974.
[38] S.R. Tzeng, C.G. Kalodimos, Dynamic activation of an allosteric regulatory protein, Nature 462 (2009) 368–372.
[39] N. Popovych, S. Sun, R.H. Ebright, C.G. Kalodimos, Dynamically driven protein allostery, Nat. Struct. Mol. Biol. 13 (2006) 831–838.
[40] B. Seelig, J.W. Szostak, Selection and evolution of enzymes from a partially randomized non-catalytic scaffold, Nature 448 (2007) 828–831.
[41] F.A.A. Mulder, R.A. de Graaf, R. Kaptein, R. Boelens, An off-resonance rotating frame relaxation experiment for the investigation of macromolecular dynamics using adiabatic rotations, J. Magn. Reson. 131 (1998) 351–357.
[42] O.W. Sorensen, G.W. Eich, M.H. Levitt, G. Bodenhausen, R.R. Ernst, Product operator formalism for the description of NMR pulse experiments, Prog. NMR Spectrosc. 16 (1984) 163–192.
[43] D. Idiyatullin, S. Michaeli, M. Garwood, Product operator analysis of the influence of chemical exchange on relaxation rates, J. Magn. Reson. 171 (2004) 330–337.
[44] D. Ban, M. Funk, R. Gulich, D. Egger, T.M. Sabo, K.F. Walter, R.B. Fenwick, K. Giller, F. Pichierri, B.L. de Groot, O.F. Lange, H. Grubmuller, X. Salvatella, M. Wolf, A. Loidl, R. Kree, S. Becker, N.A. Lakomek, D. Lee, P. Lunkenheimer, C. Griesinger, Kinetics of conformational sampling in ubiquitin, Angew. Chem. Int. Ed. Engl. 50 (2011) 11437–11440.
[45] E.L. Kovrigin, J.G. Kempf, M.J. Grey, J.P. Loria, Faithful estimation of dynamics parameters from CPMG relaxation dispersion measurements, J. Magn. Reson. 180 (2006) 93–104.
[46] O.M. Millet, J.P. Loria, C.D. Kroenke, The static magnetic field dependence of chemical exchange linebroadening defines the NMR chemical shift time scale, J. Am. Chem. Soc. 122 (2000) 2867–2877.
[47] S. Michaeli, H. Grohn, O. Grohn, D.J. Sorce, R. Kauppinen, C.S. Springer Jr., K. Ugurbil, M. Garwood, Exchange-influenced T2rho contrast in human brain images measured with adiabatic radio frequency pulses, Magn. Reson. Med. 53 (2005) 823–829.
[48] S. Mangia, T. Liimatainen, M. Garwood, I. Tkac, P.G. Henry, D. Deelchand, S. Michaeli, Frequency offset dependence of adiabatic rotating frame relaxation rate constants: relevance to MRS investigations of metabolite dynamics in vivo, NMR Biomed. 24 (2011) 807–814.
[49] S. Mangia, F. De Martino, T. Liimatainen, M. Garwood, S. Michaeli, Magnetization transfer using inversion recovery during off-resonance irradiation, Magn. Reson. Imaging 29 (2011) 1346–1350.
[50] M. Deschamps, G. Kervern, D. Massiot, G. Pintacuda, L. Emsley, P.J. Grandinetti, Superadiabaticity in magnetic resonance, J. Chem. Phys. 129 (2008) 204110.
[51] G. Pileio, M. Carravetta, M.H. Levitt, Storage of nuclear magnetization as long-lived singlet order in low magnetic field, Proc. Natl. Acad. Sci. USA 107 (2010) 17135–17139.

[52] A. Tannus, M. Garwood, Adiabatic pulses, NMR Biomed. 10 (1997) 423–434.
[53] J.P. Loria, M. Rance, A.G. Palmer 3rd, A relaxation-compensated Carr–Purcell–Meiboom–Gill sequence for characterizing chemical exchange by NMR spectroscopy, J. Am. Chem. Soc. 121 (1999) 2331–2332.
[54] Z. Luz, S. Meiboom, Nuclear magnetic resonance study of the protolysis of trimethylammonium ion in aqueous solution-order of the reaction with respect to solvent, J. Chem. Phys. 39 (1963) 366–370.
[55] M. Garwood, Y. Ke, Symmetric pulses to induce arbitrary flip angles with compensation for RF inhomogeneity and resonance offsets, J. Magn. Reson. 94 (1991) 511–525.
[56] T.L. Hwang, P.C. van Zijl, M. Garwood, Fast broadband inversion by adiabatic pulses, J. Magn. Reson. 133 (1998) 200–203.
[57] J.G. Kempf, J.Y. Jung, N.S. Sampson, J.P. Loria, Off-resonance TROSY (R1ρ-R1) for quantitation of fast exchange processes in large proteins, J. Am. Chem. Soc. 125 (2003) 12064–12065.
[58] C.D. Kroenke, J.P. Loria, L.K. Lee, M. Rance, A.G. Palmer, Longitudinal and transverse 1H–15N Dipolar/15N chemical shift anisotropy relaxation interference: unambiguous determination of rotational diffusion tensors and chemical exchange effects in biological macromolecules, J. Am. Chem. Soc. 120 (1998) 7905–7915.